

Analytical solutions to the boundary integral equation: A case of angled dendrites and paraboloids

Dmitri V. Alexandrov¹  | Peter K. Galenko^{1,2} 

¹Department of Theoretical and Mathematical Physics, Laboratory of Multi-Scale Mathematical Modeling, Ural Federal University, Ekaterinburg, Russian Federation

²Faculty of Physics and Astronomy, Friedrich Schiller University Jena, Jena, Germany

Correspondence

Peter K. Galenko, Faculty of Physics and Astronomy, Otto Schott Institute of Materials Research, Friedrich Schiller University Jena, Jena, Germany.
Email: peter.galenko@uni-jena.de

Communicated by: I. Nizovtseva

Funding information

Deutsches Zentrum für Luft- und Raumfahrt, Grant/Award Number: 50WM1941; Ministry of Science and Higher Education of the Russian Federation, Grant/Award Number: FEUZ-2020-0057; German Space Center Space Management, Grant/Award Number: 50WM1941

The boundary integral equation is solved analytically in the case of two- and three-dimensional growth of angled dendrites and arbitrary parabolic/paraboloidal solid/liquid interfaces. The undercooling of a binary melt and the solute concentration at the phase transition boundary are found. The theory under consideration has a potential impact in describing more complex growth shapes and interfaces.

KEYWORDS

boundary integral, dendrite, model, solidification

MSC CLASSIFICATION

82B26

1 | INTRODUCTION

The boundary integral equation was derived for the first time by Nash and Glicksman^{1,2} for the pure thermal problem of the solid–liquid interface evolution. Their theory was developed by Langer and Turski^{3,4} in describing the evolutionary behavior of ‘solid–liquid’, ‘solid–solid’, and ‘fluid–fluid’ interface functions in the case of a chemical diffusion problem. This theory was recently extended for propagating interfaces in a binary non-isothermal mixture.^{5,6} The boundary integral method was generalized for the rapid crystallization conditions when the solute transport is described by a hyperbolic-type diffusion equation in recently published theory.^{7,8}

It is well-known that the boundary integral equation completely determines the nonlinear dynamics of the solid–liquid interface when considering one-component and binary melt solidification processes.^{3–8} In addition, this equation enables us to select a stable mode of dendritic growth, that is, to find a relation connecting the steady-state tip velocity and tip radius of dendritic crystal.^{9–11} What is more, the boundary integral contains all the information about morphology, instability, and pattern formation of propagating interfaces, and thus, it defines the morphological diversity of growth shapes existing in nature and various physical applications.¹² In the present article, we find an analytical solution in the

This is an open access article under the terms of the Creative Commons Attribution License, which permits use, distribution and reproduction in any medium, provided the original work is properly cited.

© 2020 The Authors. *Mathematical Methods in the Applied Sciences* published by John Wiley & Sons Ltd.

form of parabolic and linear functions following from the boundary integral theory that reflects the growing shapes and morphologies in binary systems.

2 | THE MODEL

The phase transition interface ζ dividing the solid and liquid material when describing the steady-state crystallization process in a binary melt takes the form⁵⁻⁷

$$-\frac{Q}{m_0 c_p} \left[\Delta - \frac{d_c}{\rho} K - \beta V - I_\zeta^T \right] - C_{l\infty} = I_\zeta^C, \quad (1)$$

where Q stands for the latent heat of solidification, m_0 is the liquidus slope, c_p represents the specific heat, $\Delta = (T_f - T_{l\infty}) c_p / Q$ expresses the melt undercooling with T_f being the phase transformation temperature corresponding to the planar front, d_c is the anisotropic capillary length, K is the curvature of solid–liquid boundary, ρ is a characteristic length scale of a growing shape, β is the kinetic coefficient of anisotropic growth, V is the steady-state growth rate, and $T_{l\infty}$ and $C_{l\infty}$ are the temperature and solute concentration in the liquid phase far from the growing shape. Note that curvature K of the solid–liquid boundary in the two- and three-dimensional geometries can be written out as^{6,7}

$$K(\zeta) = \begin{cases} -\frac{\partial^2 \zeta / \partial x^2}{[1 + (\partial \zeta / \partial x)^2]^{3/2}}, & \text{two dimensions} \\ -\nabla \cdot \left[\frac{\nabla \zeta}{\sqrt{1 + (\nabla \zeta)^2}} \right], & \text{three dimensions} \end{cases} \quad (2)$$

The boundary integrals I_ζ^T and I_ζ^C describing the temperature and concentration contributions are determined by the interface function $\zeta(x, y)$ and take the form⁵⁻⁷

$$\begin{aligned} I_\zeta^T &= P_T \int_0^\infty \frac{d\tau}{2\pi\tau} \int_{-\infty}^\infty \exp \left[-\frac{P_T}{2\tau} \Sigma(x, x_1, \tau) \right] dx_1, \\ I_\zeta^C &= (1 - k_0) P_C \int_0^\infty \frac{d\tau}{2\pi\tau} \int_{-\infty}^\infty C_i(x_1) \exp \left[-\frac{P_C}{2\tau} \Sigma(x, x_1, \tau) \right] dx_1, \\ \Sigma(x, x_1, \tau) &= (x - x_1)^2 + [\zeta(x) - \zeta(x_1) + \tau]^2, \end{aligned} \quad (3)$$

in the two-dimensional geometry and

$$\begin{aligned} I_\zeta^T &= P_T^{3/2} \int_0^\infty \frac{d\tau}{(2\pi\tau)^{3/2}} \int_{-\infty}^\infty \int_{-\infty}^\infty \exp \left[-\frac{P_T}{2\tau} \Sigma(\mathbf{x}, \mathbf{x}_1, \tau) \right] d^2 x_1, \\ I_\zeta^C &= (1 - k_0) P_C^{3/2} \int_0^\infty \frac{d\tau}{(2\pi\tau)^{3/2}} \int_{-\infty}^\infty \int_{-\infty}^\infty C_i(\mathbf{x}_1) \exp \left[-\frac{P_C}{2\tau} \Sigma(\mathbf{x}, \mathbf{x}_1, \tau) \right] d^2 x_1, \\ \Sigma(\mathbf{x}, \mathbf{x}_1, \tau) &= |\mathbf{x} - \mathbf{x}_1|^2 + [\zeta(\mathbf{x}) - \zeta(\mathbf{x}_1) + \tau]^2, \end{aligned} \quad (4)$$

in the three-dimensional geometry. Here, $P_C = \rho V / (2D_C)$ and $P_T = \rho V / (2D_T)$ are the solutal (chemical) and thermal Péclet numbers, respectively; D_C is the diffusion coefficient; D_T is the thermal diffusivity; k_0 stands for the equilibrium segregation coefficient; and $C_i = C_{l\infty} + I_\zeta^C$ is the concentration at the solid–liquid interface. Note that the variables in integrals (3) and (4) are dimensionless⁵⁻⁷ (the dimensional form can be found by means of the characteristic length ρ).

3 | ANALYTICAL SOLUTIONS

3.1 | Parabolic/paraboloidal growth shapes

First, let us seek for a solution of the boundary integral equation (1) in the form of a quadratic function in the two-dimensional geometry as

$$\zeta(x) = ax^2 + bx + c, \quad (5)$$

where a , b , and c represent the constant coefficients and $a < 0$ if the branches of the parabola are directed downwards. Substituting this function into the integral I_ζ^T from Equation (3) and changing the variable of integration (ω instead of τ) as

$$\omega = \frac{(x - x_1)^2}{2\tau},$$

we get

$$I_\zeta^T = \frac{P_T}{2\pi} \int_0^\infty \frac{d\omega}{\omega} \int_{-\infty}^\infty \exp \left[-P_T \omega \left(1 + \left(a(x + x_1) + b + \frac{x - x_1}{2\omega} \right)^2 \right) \right] dx_1. \quad (6)$$

Now introducing new variable

$$z = -\sqrt{P_T \omega} \left(a(x + x_1) + b + \frac{x - x_1}{2\omega} \right),$$

one can evaluate integral (6) with respect to x_1 and obtain

$$I_\zeta^T = -\frac{\sqrt{P_T}}{2\sqrt{\pi}} \int_0^\infty \frac{\exp(-P_T \omega) d\omega}{\sqrt{\omega}(a\omega - 1/2)}. \quad (7)$$

This integral can be easily evaluated if $a = 0$ as

$$I_\zeta^T = 1, \quad a = 0. \quad (8)$$

Here, the following expression is taken into account¹³:

$$\int_0^\infty \frac{\exp(-q\alpha)}{\sqrt{\alpha}} d\alpha = \sqrt{\frac{\pi}{q}}, \quad q > 0. \quad (9)$$

Let us now consider the case $a \neq 0$ and bring integral (7) into a form that is tabulated

$$I_\zeta^T = 1 - \sqrt{\frac{P_T}{\pi}} a \int_0^\infty \frac{\sqrt{\omega} \exp(-P_T \omega) d\omega}{a\omega - 1/2}. \quad (10)$$

Now keeping in mind that¹³

$$\int_u^\infty \frac{\sqrt{\alpha - u}}{\alpha} \exp(-\mu\alpha) d\alpha = \sqrt{\frac{\pi}{\mu}} \exp(-\mu u) - \pi \sqrt{u} \operatorname{erfc}(\sqrt{u\mu}), \quad u > 0, \quad \operatorname{Re}(\mu) > 0,$$

we finally obtain from (10)

$$I_\zeta^T = \begin{cases} \sqrt{-\frac{\pi P_T}{2a}} \exp\left(-\frac{P_T}{2a}\right) \operatorname{erfc}\left(\sqrt{-\frac{P_T}{2a}}\right), & a < 0 \\ 1, & a = 0 \end{cases}. \quad (11)$$

Setting $a = -1/2$, we have from (11) the previously found result^{6,8}

$$I_{\zeta}^T = P_T \exp(P_T) \int_1^{\infty} \frac{\exp(-P_T v)}{\sqrt{v}} dv, \quad (12)$$

which coincides with expressions (30)⁶ and (5.1).⁸

The solutal contribution I_{ζ}^C entering in the boundary integral (1) can be easily evaluated by analogy with the integral I_{ζ}^T . To do this, we just replace P_T by P_C and take into account the constant factor $(1 - k_0)C_i$. So, we have from expressions (3) in the two-dimensional case

$$I_{\zeta}^C = (1 - k_0)C_i f(P_C), \quad (13)$$

$$f(P_C) = \begin{cases} \sqrt{-\frac{\pi P_C}{2a}} \exp\left(-\frac{P_C}{2a}\right) \operatorname{erfc}\left(\sqrt{-\frac{P_C}{2a}}\right), & a < 0 \\ 1, & a = 0 \end{cases}. \quad (14)$$

Now substituting I_{ζ}^C into expression $C_i = C_{i\infty} + I_{\zeta}^C$, we come to the interfacial concentration, which reads as

$$C_i = \frac{C_{i\infty}}{1 - (1 - k_0)f(P_C)}. \quad (15)$$

Note that expression (15) coincides with expressions (34)⁶ and (5.8)⁸ in the limiting case $a = -1/2$.

Now we consider the three-dimensional case when the interface function represents a paraboloid of revolution given by

$$\zeta(x, y) = a(x^2 + y^2) + b(x + y) + c, \quad (16)$$

where $a < 0$, b , and c are the constant coefficients. To evaluate the thermal integral I_{ζ}^T in (4) we replace the variables ω and y_1 by τ and z_1 by means of the following substitutions:

$$\omega = \frac{(x - x_1)^2}{2\tau}, \quad y - y_1 = (x - x_1)z_1. \quad (17)$$

As a result, the thermal integral simplifies as

$$I_{\zeta}^T = -\frac{1}{2} \left(\frac{P_T}{\pi}\right)^{3/2} \int_0^{\infty} \frac{d\omega}{\sqrt{\omega}} \int_{-\infty}^{\infty} \frac{\exp[-P_T \omega(1 + z_1^2)] dz_1}{a + az_1^2 - (2\omega)^{-1}} \int_{-\infty}^{\infty} \exp(-P_T \omega u^2) du, \quad (18)$$

where $a < 0$ and

$$u = a(x + x_1) + b(1 + z_1) + az_1 [2y - (x - x_1)z_1] + \frac{x - x_1}{2\omega}.$$

Now evaluating two last integrals in (18) and taking into account that¹³

$$\int_0^{\infty} \frac{\exp(-\mu^2 v^2) dv}{v^2 + \beta^2} = \frac{\pi}{2\beta} \operatorname{erfc}(\beta\mu) \exp(\beta^2 \mu^2),$$

we have

$$I_{\zeta}^T = -\frac{P_T}{a} \exp\left(-\frac{P_T}{2a}\right) \int_{1/\sqrt{-2a}}^{\infty} \frac{\operatorname{erfc}\left[\sqrt{P_T} w\right] dw}{\sqrt{w^2 + (2a)^{-1}}}, \quad (19)$$

where $w = \sqrt{\omega - (2a)^{-1}}$. We use the method of differentiation and integration by the parameter $\alpha = \sqrt{P_T}$ to evaluate integral (19). To do this, we consider the integral

$$J(\alpha) = \int_{1/\sqrt{-2a}}^{\infty} \frac{\operatorname{erfc}[aw] dw}{\sqrt{w^2 + (2a)^{-1}}}.$$

Its differentiation gives

$$J'(\alpha) = -\frac{\exp[\alpha^2(1 + (2a)^{-1})]}{\sqrt{\pi}} \int_1^{\infty} \frac{\exp[-\alpha^2\gamma] d\gamma}{\sqrt{\gamma-1}},$$

where $\gamma = w^2 + 1 + (2a)^{-1}$. The last integral can be evaluated in terms of elementary functions as¹³ $\sqrt{\pi} \exp(-\alpha^2)/\alpha$. Taking this into account, we obtain

$$J'(\alpha) = -\frac{1}{\alpha} \exp\left[\frac{\alpha^2}{2a}\right].$$

Now keeping in mind that $J(\alpha) \rightarrow 0$ as $\alpha \rightarrow \infty$, we have after integration

$$J(\alpha) = \int_{\alpha}^{\infty} \exp\left[\frac{v^2}{2a}\right] \frac{dv}{v}.$$

Now substituting this result into expression (19) and replacing the variable of integration as $v = \sqrt{P_T\eta}$, we finally obtain the thermal integral

$$I_{\zeta}^T = -\frac{P_T}{2a} \exp\left[-\frac{P_T}{2a}\right] \int_1^{\infty} \exp\left[\frac{P_T\eta}{2a}\right] \frac{d\eta}{\eta}. \quad (20)$$

Note that expression (20) coincides with expressions (31)⁶ and (5.5)⁸ in the case $a = -1/2$.

In the case $a = 0$, the thermal integral can be easily found from expression (18). Indeed, keeping in mind (9), we conclude $I_{\zeta}^T = 1$ at $a = 0$. Thus, we have in the three-dimensional case

$$I_{\zeta}^T = \begin{cases} -\frac{P_T}{2a} \exp\left[-\frac{P_T}{2a}\right] \int_1^{\infty} \exp\left[\frac{P_T\eta}{2a}\right] \frac{d\eta}{\eta}, & a < 0 \\ 1, & a = 0 \end{cases}. \quad (21)$$

To find the solutal integral I_{ζ}^C in the three-dimensional growth geometry, we should again replace P_T by P_C and take into consideration the constant factor $(1 - k_0)C_i$. As a result, we have from expression (4) in the three-dimensional case

$$I_{\zeta}^C = (1 - k_0)C_i g(P_C), \quad (22)$$

$$g(P_C) = \begin{cases} -\frac{P_C}{2a} \exp\left[-\frac{P_C}{2a}\right] \int_1^{\infty} \exp\left[\frac{P_C\eta}{2a}\right] \frac{d\eta}{\eta}, & a < 0 \\ 1, & a = 0 \end{cases}. \quad (23)$$

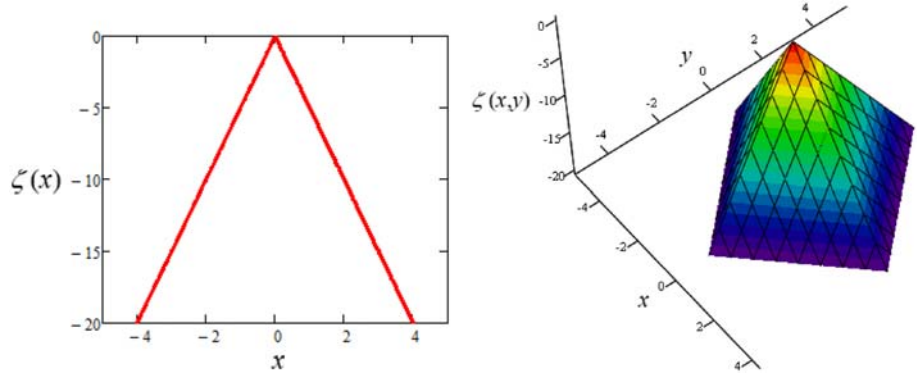
Substitution of I_{ζ}^C into $C_i = C_{i\infty} + I_{\zeta}^C$ gives the interfacial concentration in the case of three-dimensional growth

$$C_i = \frac{C_{i\infty}}{1 - (1 - k_0)g(P_C)}. \quad (24)$$

Note that expression (24) again coincides with expressions (34)⁶ and (5.8)⁸ in the limiting case $a = -1/2$.

The undercooling Δ is defined by Equation (1). If we are dealing with the planar front when $a = 0$, the solid-liquid interface curvature $K(\zeta)$ becomes zero and Equation (1) is satisfied automatically. If the growth shape is parabolic

FIGURE 1 A sketch of two-dimensional angled dendrite (left panel) and three-dimensional angled dendrite (right panel), which are given by equations $\zeta(x) = a|x|$ and $\zeta(x, y) = a(|x| + |y|)$, respectively, with $a = -5$ [Colour figure can be viewed at wileyonlinelibrary.com]



(or paraboloidal), the interface curvature, generally speaking, does not vanish. Therefore, such shapes can satisfy this equation only approximately when the term proportional to $K(\zeta)$ in Equation (1) is much less than other contributions. This occurs, for example, if the factor d_c/ρ is small enough too. Keeping this in mind, we arrive at the undercooling of a binary melt

$$\Delta = \beta V + I_\zeta^T - \frac{m_0 c_p}{Q} (I_\zeta^C + C_{l\infty}). \quad (25)$$

3.2 | Angled dendrite-like growth shapes

From the boundary layer model¹⁴ and from the cellular automata modeling,¹⁵ it is known that the dendrites can have an angled shape of their tips. This angled shape of dendrite can also be obtained from the presently developing boundary integral theory.

Consider the case of two-dimensional angled dendrite growing in a binary mixture. Its shape $\zeta(x) = a|x| + b$ is illustrated in Figure 1 (here, $a < 0$ and b are constants). For the sake of convenience, the thermal integral I_ζ^T from (3) can be divided into two parts as

$$I_\zeta^T = P_T \int_0^\infty \frac{d\tau}{2\pi\tau} \left(\int_0^\infty + \int_{-\infty}^0 \right) \exp \left[-\frac{P_T}{2\tau} \Sigma(x, x_1, \tau) \right] dx_1. \quad (26)$$

At first, we evaluate the first part, where $\zeta(x_1) = ax_1 + b$, and $\Sigma(x, x_1, \tau)$ becomes

$$\Sigma(x, x_1, \tau) = (x - x_1)^2 + [a(x - x_1) + \tau]^2.$$

Introducing the new variable $\omega = (x - x_1)^2 / (2\tau)$ instead of τ , then replacing x_1 by u as $u = -\sqrt{P_T\omega} [a + (x - x_1)/(2\omega)]$, and omitting all mathematical manipulations, we arrive at the first contribution to I_ζ^T in (26), which reads as

$$\frac{\sqrt{P_T}}{2\sqrt{\pi}} \int_0^\infty \frac{\exp(-P_T\omega)}{\sqrt{\omega}} \operatorname{erfc} \left[-\sqrt{P_T\omega} \left(a + \frac{|x|}{2\omega} \right) \right] d\omega. \quad (27)$$

To evaluate the second contribution in (26), we should take into account that

$$\zeta(x_1) = -ax_1 + b, \quad u = \sqrt{P_T\omega} \left(\frac{x - x_1}{2\omega} - a \right).$$

As a result, we come to the same contribution. Therefore, I_ζ^T is equal to double expression (27) and reads as

$$I_\zeta^T = \sqrt{\frac{P_T}{\pi}} \int_0^\infty \frac{\exp(-P_T\omega)}{\sqrt{\omega}} \operatorname{erfc} \left[-\sqrt{P_T\omega} \left(a + \frac{|x|}{2\omega} \right) \right] d\omega. \quad (28)$$

In the vicinity of dendritic vertex where $|x|$ is small enough, we have

$$I_{\zeta}^T = \sqrt{\frac{P_T}{\pi}} \int_0^{\infty} \frac{\exp(-P_T \omega)}{\sqrt{\omega}} \operatorname{erfc}\left(-a\sqrt{P_T \omega}\right) d\omega = \frac{2}{\pi} \arctan\left(-\frac{1}{a}\right). \quad (29)$$

The last expression (29) is obtained by the method of differentiation with respect to the parameter a , integration over ω , and then over a with allowance for $I_{\zeta}^T \rightarrow 0$ as $a \rightarrow -\infty$.

Note that the integral I_{ζ}^C defined in (3) may be found by analogy with I_{ζ}^T as $I_{\zeta}^C = (1 - k_0)C_i I_{\zeta}^T$. Keeping in mind that $C_i = I_{\zeta}^C + C_{i\infty}$, we come to

$$I_{\zeta}^C = \frac{(1 - k_0)C_{i\infty} I_{\zeta}^T}{1 - (1 - k_0)I_{\zeta}^T}, \quad a < 0. \quad (30)$$

Let us estimate the integral I_{ζ}^T from (4) in the three-dimensional case (see Figure 1) taking into account that $\zeta(x, y) = a(|x| + |y|) + b$ ($a < 0$ and b are constants). To do this, we calculate four contributions of the integral I_{ζ}^T in (4). The first contribution corresponds to the following function $\zeta(x, y) = a(x + y) + b$ ($x > 0, y > 0$), and

$$\Sigma(x, y) = (x - x_1)^2 + (y - y_1)^2 + [a(x - x_1) + a(y - y_1) + \tau]^2.$$

Changing τ by ω and y_1 by z_1 using substitutions

$$\tau = \frac{(x - x_1)^2}{2\omega}, \quad y_1 = y + (x - x_1)z_1,$$

we arrive at the first contribution in the form of

$$\frac{P_T^{3/2}}{2\pi^{3/2}} \int_0^{\infty} \int_0^{\infty} \int_{-y/(x-x_1)}^{\infty} \exp\left\{-P_T \omega \left[1 + z_1^2 + \left(a - az_1 + \frac{x - x_1}{2\omega}\right)^2\right]\right\} dz_1 dx_1 \frac{d\omega}{\sqrt{\omega}}. \quad (31)$$

Changing now z_1 by u

$$u = \sqrt{1 + a^2} z_1 - \chi(x_1, \omega), \quad \chi(x_1, \omega) = \frac{a(a + (x - x_1)/(2\omega))}{\sqrt{1 + a^2}},$$

we get from (31)

$$\frac{P_T}{4\pi\sqrt{1 + a^2}} \int_0^{\infty} \left\{ \int_0^{\infty} \exp[-P_T(1 + \kappa(x_1, \omega))\omega] \operatorname{erfc}\left[-\sqrt{P_T \omega} \left(\frac{\sqrt{1 + a^2} y}{x - x_1} + \chi(x_1, \omega)\right)\right] dx_1 \right\} \frac{d\omega}{\omega}. \quad (32)$$

Here, $\kappa(x_1, \omega) = \chi^2(x_1, \omega)/a^2$.

Three other terms to I_{ζ}^T in expression (4) where x and y have various signs may be determined in the same manner. All of these terms are identical to expression (32). Keeping this in mind, we multiply (32) by 4 and obtain the final expression.

Let us now pay our attention to the vertex zone where $x \rightarrow 0$ and $y \rightarrow 0$. In this case, we obtain from (32)

$$I_{\zeta}^T = \frac{P_T}{\pi\sqrt{1 + a^2}} \int_0^{\infty} \left\{ \int_0^{\infty} \exp[-P_T(1 + \tilde{\kappa}(x_1, \omega))\omega] \operatorname{erfc}\left[-\sqrt{P_T \omega} \tilde{\chi}(x_1, \omega)\right] dx_1 \right\} \frac{d\omega}{\omega}, \quad (33)$$

where

$$\tilde{\chi}(x_1, \omega) = \frac{a(a - x_1/(2\omega))}{\sqrt{1 + a^2}}, \quad \tilde{\kappa}(x_1, \omega) = \frac{\tilde{\chi}^2(x_1, \omega)}{a^2}.$$

Replacing the variables of integration accordingly to

$$\omega' = P_T \omega, \quad x'_1 = P_T x_1,$$

we find from (33)

$$I_\zeta^T = \frac{1}{\pi \sqrt{1+a^2}} \int_0^\infty \left\{ \int_0^\infty \exp [-(1+\kappa')\omega'] \operatorname{erfc} [-\sqrt{\omega'} \chi'] dx'_1 \right\} \frac{d\omega'}{\omega'}, \quad (34)$$

$$\chi' (x'_1, \omega') = \frac{a (a - x'_1/(2\omega'))}{\sqrt{1+a^2}}, \quad \kappa' (x'_1, \omega') = \frac{\chi'^2 (x'_1, \omega')}{a^2}, \quad a < 0.$$

The integral I_ζ^C can be evaluated by analogy with I_ζ^T and takes the form

$$I_\zeta^C = \frac{(1-k_0) C_{l\infty} I_\zeta^T}{1 - (1-k_0) I_\zeta^T}. \quad (35)$$

Note that formulas (34) and (35) characterizing the three-dimensional angled crystal are independent of the Péclet numbers P_T and P_C . Let us also especially emphasize that the melt undercooling is determined by Equation (1) with I_ζ^T and I_ζ^C given by expressions (29) and (30) in two-dimensional angled dendrite or (34) and (35) in three-dimensional angled dendrite (see Figure 1).

4 | CONCLUDING REMARKS

In summary, generalized analytical solutions for the parabolic/paraboloidal growing shapes and angled-like dendrites in two/three spatial dimensions are found analytically on the basis of the boundary integral theory. These solutions allowed us to get the thermal and concentration integrals entering in the Gibbs–Thomson condition (1) that determines the undercooling in a binary liquid ahead of the growing curved solid–liquid boundaries. The theory under consideration can be extended to find a stable growth mode of angled-like dendrites in the spirit of previously developed solvability theory.^{9–11} In addition, this approach can be used in describing the same shapes of solid/liquid interfaces growing in various solidification conditions (rapid crystallization, solidification with a mushy layer, ternary systems, convective mechanism of heat and mass transfer, and solid–solid and liquid–liquid interface propagation may be mentioned^{16–25}).

The presently developed theory can also be used in studying the morphology of more complex solid/liquid shapes and interfaces propagating into undercooled one-component and binary liquids.

ACKNOWLEDGEMENTS

This work was supported by the Ministry of Science and Higher Education of the Russian Federation (project number FEUZ-2020-0057) and the German Space Center Space Management (contract number 50WM1941).

AUTHOR CONTRIBUTIONS

The authors contributed equally to the present research article.

CONFLICT OF INTEREST

The authors declare no potential conflict of interests.

ORCID

Dmitri V. Alexandrov  <https://orcid.org/0000-0002-6628-745X>

Peter K. Galenko  <https://orcid.org/0000-0003-2941-7742>

REFERENCES

1. Nash GE. Capillary-limited, steady state dendritic growth. Part I. Theoretical development. NRL Report. 1974;1974;7679.
2. Nash GE, Glicksman ME. Capillary-limited steady-state dendritic growth I. Theoretical development. *Acta Metall.* 1974;22:1283-1290.
3. Langer JS, Turski LA. Studies in the theory of interface stability—I. Stationary symmetric model. *Acta Metall.* 1977;25:1113-1119.
4. Langer JS. Studies in the theory of interface stability—II. Moving symmetric model. *Acta Metall.* 1977;25:1121-1137.
5. Brener EA, Melnikov VI. Pattern selection in two-dimensional dendritic growth. *Adv Phys.* 1991;40:53-97.
6. Alexandrov DV, Galenko PK. Boundary integral approach for propagating interfaces in a binary non-isothermal mixture. *Physica A.* 2017;469:420-428.
7. Alexandrov DV, Galenko PK. Selected mode for rapidly growing needle-like dendrite controlled by heat and mass transport. *Acta Mater.* 2017;137:64-70.
8. Galenko PK, Alexandrov DV, Titova EA. The boundary integral theory for slow and rapid curved solid/liquid interfaces propagating into binary systems. *Phil Trans R Soc A.* 2018;376:20170218.
9. Barbieri A, Langer JS. Predictions of dendritic growth rates in the linearized solvability theory. *Phys Rev A.* 1989;39:5314-5325.
10. Ben Amar M, Pelcé P. Impurity effect on dendritic growth. *Phys Rev A.* 1989;39:4263-4269.
11. Ben Amar M. Dendritic growth rate at arbitrary undercooling. *Phys Rev A;* 41:2080-2092.
12. Alexandrov DV, Galenko PK. The shape of dendritic tips. *Phil Trans R Soc A.* 2020;378:20190243.
13. Gradshteyn IM. *Tables of Integrals, Series, and Products.* New York: Academic Press; 2007.
14. Brener EA, Temkin DE. Dendritic growth at deep undercooling and transition to planar front. *Europhys Lett.* 1989;10:171-175.
15. Galenko PK, Krivilyov MD, Buzilov SV. Bifurcations in a sidebranch surface of a free-growing dendrite. *Phys Rev E.* 1997;55:611-619.
16. Alexandrov DV, Galenko PK, Toropova LV. Thermo-solutal and kinetic modes of stable dendritic growth with different symmetries of crystalline anisotropy in the presence of convection. *Phil Trans R Soc A.* 2018;376:20170215.
17. Alexandrov DV, Bashkirtseva IA, Ryashko LB. Nonlinear dynamics of mushy layers induced by external stochastic fluctuations. *Phil Trans R Soc A.* 2018;376:20170216.
18. Alexandrov DV, Nizovtseva IG. On the theory of crystal growth in metastable systems with biomedical applications: protein and insulin crystallization. *Phil Trans R Soc A.* 2019;377:20180214.
19. Karma A, Rappel WJ. Phase-field model of dendritic sidebranching with thermal noise. *Phys Rev E.* 1999;60:3614-3625.
20. Horvay G, Cahn JW. Dendritic and spheroidal growth. *Acta Metall.* 1961;9:695-705.
21. Alexandrov DV, Danilov DA, Galenko PK. Selection criterion of a stable dendrite growth in rapid solidification. *Int J Heat Mass Trans.* 2016;101:789-799.
22. Alexandrov DV, Galenko PK. Thermo-solutal and kinetic regimes of an anisotropic dendrite growing under forced convective flow. *Phys Chem Chem Phys.* 2015;17:19149-19161.
23. Danilov D, Nestler B. Dendritic to globular morphology transition in ternary alloy solidification. *Phys Rev Lett.* 2004;93:215501.
24. Alexandrova IV, Alexandrov DV. Dynamics of particulate assemblages in metastable liquids: a test of theory with nucleation and growth kinetics. *Phil Trans R Soc A.* 2020;378:20190245.
25. Alexandrov DV, Galenko PK. Selection criterion of stable mode of dendritic growth with n-fold symmetry at arbitrary Peclet numbers with a forced convection. In: Gutschmidt S, Hewett JN, Sellier M, eds. *IUTAM Symposium on Recent Advances in Moving Boundary Problems in Mechanics*, IUTAM Bookseries 34.: Springer; 2019:203-215.

How to cite this article: Alexandrov DV, Galenko PK. Analytical solutions to the boundary integral equation: a case of angled dendrites and paraboloids. *Math Meth Appl Sci.* 2020;1–9. <https://doi.org/10.1002/mma.6570>